

Luminescence kinetics of iodine-doped silver bromide crystals: concentration and excitation intensity dependences

This article has been downloaded from IOPscience. Please scroll down to see the full text article.

1996 J. Phys.: Condens. Matter 8 6445

(<http://iopscience.iop.org/0953-8984/8/35/013>)

View [the table of contents for this issue](#), or go to the [journal homepage](#) for more

Download details:

IP Address: 171.66.16.206

The article was downloaded on 13/05/2010 at 18:35

Please note that [terms and conditions apply](#).

Luminescence kinetics of iodine-doped silver bromide crystals: concentration and excitation intensity dependences

L Nagli and A Katzir

Raymond and Beverly Sackler Faculty of Exact Science, School of Physics and Astronomy,
Tel-Aviv University, Tel-Aviv 69978, Israel

Received 26 October 1995, in final form 13 March 1996

Abstract. The decay kinetics of iodine bound excitons in AgBr:I crystals have been studied. Luminescence kinetics, quenching and changes in kinetics are observed to depend on the iodine concentration and the excitation intensity. These observations are discussed in terms of donor–donor and donor–acceptor interactions. The probabilities of energy migration via iodide ions and probability of luminescence quenching are estimated.

1. Introduction

AgBr:I crystals, at low temperatures, show an intense luminescence at 2.5 eV when excited by energy at the indirect absorption edge. At relatively low iodine concentrations this luminescence has been attributed to the radiative decay of iodine-bound excitons [1–7]. At higher iodine concentrations the 2.5 eV emission band shifts to a longer wavelength and is assigned to donor–acceptor recombination [8]. At low-power pulse excitation, the luminescence decays exponentially. At temperatures near 4 K and low concentrations (10^{18} cm⁻³ or less) the decay time of this luminescence is about 17 μ s [1, 2, 9]. At higher iodine concentrations the kinetics of the luminescence are more complicated [5].

High-intensity excitation luminescence has been studied mainly in pure AgBr crystals in order to investigate excitonic molecules and droplets of the electron–hole liquid [10–12] in such crystals.

The main purpose of the present work is to investigate the iodine-bound exciton luminescence in AgBr:I crystals under high-power density excitation. In particular, we examine the dependence of the luminescence kinetics of the excitation power density in order to clarify the interactions between iodine-bound excitons in AgBr crystals.

2. Experimental details

Pure and I-doped crystals were grown from the melt in our laboratory by the Bridgman–Stockbarger technique using pure starting materials.

The iodine concentration was assumed to be equal to the AgI concentration added to the AgBr melt. We have also checked the iodine concentration with a method proposed by Moser and Lyu [1] using the ratio of the luminescence band at 2.5 eV to that at 2.12 eV and some spectra shown in the literature and have found good agreement with the assumption.

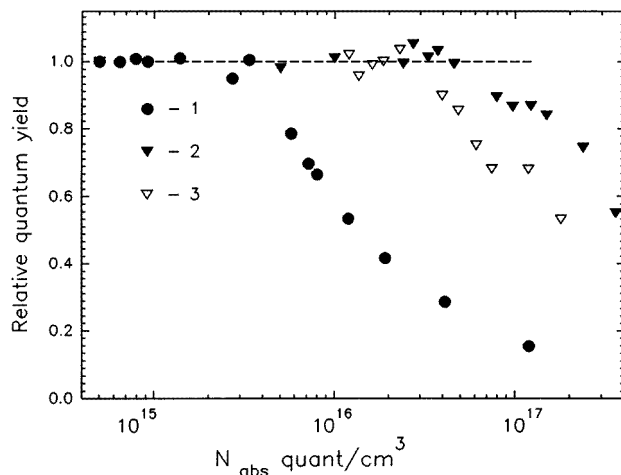


Figure 1. Dependence of the relative quantum yield of the iodine-bound exciton luminescence at 20 K on the concentration of absorbed quanta at 440 nm in AgBr crystals: ●, iodine concentration of $4 \times 10^{15} \text{ cm}^{-3}$; ▼, iodine concentration of $1.6 \times 10^{17} \text{ cm}^{-3}$; ▽, iodine concentration of $4 \times 10^{16} \text{ cm}^{-3}$.

The residual iodide ion concentration in nominally pure AgBr crystals was estimated to be $4 \times 10^{15} \text{ cm}^{-3}$; doped samples contained 4×10^{16} , 1.6×10^{17} , 2×10^{18} and $2 \times 10^{19} \text{ cm}^{-3}$ of iodide ions.

Discs of diameter 8 mm and thickness 3 mm were cut and polished and mounted in a cryostat (CTI-Cryogenics). Luminescence generally was measured at about 20 K. The steady-state luminescence was transmitted through a Hilger–Watts quartz prism monochromator and detected with a photomultiplier (EMI 9558Q; S-20). Continuous excitation of the luminescence was produced by a high-pressure Xe lamp which was monitored with a small Airy monochromator. A pulsed nitrogen laser (LSI Science, Inc., model VSL-337ND) or a pulsed dye laser (LSI Science, Inc., model DLM-220) was used for high-power pulsed excitation. In the case of the nitrogen laser the excitation was at 337 nm (3.68 eV), with a maximum pulse energy of 400 μJ and a pulse duration of 3 ns. In the case of the dye laser, a Coumarin 440 dye with a maximum pulse energy of 60 μJ at 440 nm (2.82 eV) and pulse duration of 3 ns was used. The laser output was focused on the crystal surface to a spot diameter of about 2 mm in the case of N_2 excitation and about 0.5 mm in the case of dye laser excitation. To vary the excitation power density a set of neutral glass density filters was used. For extremely low-level excitation, the laser beams were defocused. For measurements of the luminescence pulses the photomultiplier output was fed into a digital processing oscilloscope (HP model 54602A). The output signal was averaged over 256 pulses. The time resolution of the detection system was about 20 ns. The recorded emission spectra were corrected for the relative spectral sensitivity of the photomultiplier and the dispersion of the monochromator.

To analyse our results it is necessary to know the concentration of the electron–hole pairs or free excitons created by the excitation. This concentration is proportional to the volume density N_{abs} of the absorbed quanta which may be determined from

$$N_{abs} = N_0 \alpha(\lambda) [1 - \exp(-\alpha(\lambda)d)] \quad (1)$$

where N_0 is the surface density of the exciting quanta, α is the absorption coefficient at the

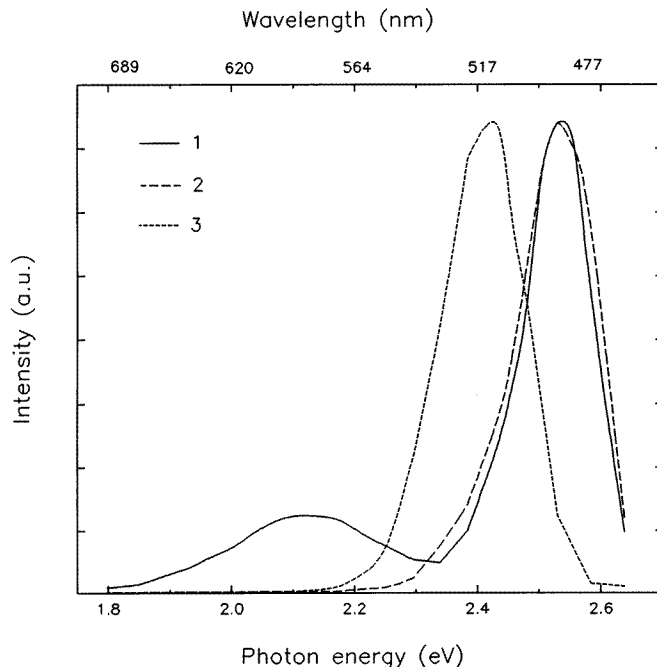


Figure 2. Steady-state luminescence spectra of AgBr crystals at 20 K with various iodine concentrations (a.u., arbitrary units): —, $4 \times 10^{15} \text{ cm}^{-3}$; ---, $1.6 \times 10^{17} \text{ cm}^{-3}$; - · - · -, $2 \times 10^{18} \text{ cm}^{-3}$. Excitation was by a Xe lamp at 425 nm.

wavelength λ and d is the thickness of the sample. The absorption coefficient at 440 nm for crystals activated with iodine concentration of 2×10^{15} – $2 \times 10^{18} \text{ cm}^{-3}$ from 10 – 40 cm^{-1} [2, 8]. At 337 nm the absorption coefficient is about $2 \times 10^3 \text{ cm}^{-1}$ [4]. Therefore the maximum volume density of the absorbed quanta for 440 nm excitation is in the range 7×10^{17} – $3 \times 10^{18} \text{ cm}^{-3}$. For 337 nm excitation this value is about $3 \times 10^{20} \text{ cm}^{-3}$. The dependences of the relative quantum yield of the luminescence on the volume excitation densities show a reduction in the quantum yield at concentrations of absorbed quanta, which depends on the iodine concentration in the sample (figure 1). The value of the absorbed quanta concentration at which this reduction begins apparently coincides with the iodine concentration in the samples. This confirmed our estimated values of the concentration of the absorbed quanta.

3. Experimental results

The experimental results of this work are divided into two parts. The first deals with measurements of luminescence kinetics under low-power pulse excitation intensity. The second part deals with the high-power excitation effects on iodine-bound exciton luminescence.

Typical steady-state luminescence spectra of nominally pure and iodine activated AgBr crystals excited by a 440 nm Xe lamp light are shown in figure 2. An emission band appears at 2.55 eV, with a weaker band at 2.12 eV in lightly doped AgBr crystals. Increasing the concentration of iodine up to $2 \times 10^{17} \text{ cm}^{-3}$ results in an increase in the intensity of the

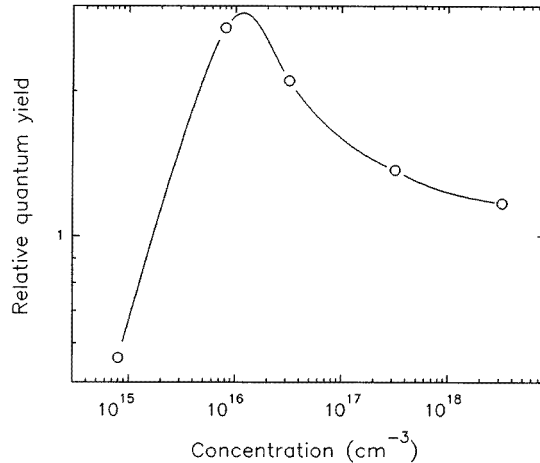


Figure 3. Dependence of the relative quantum yield of AgBr crystal luminescence at 20 K on iodine concentration with excitation by 440 nm light pulses with a surface quantum density of about 10^{14} cm^{-2} .

luminescence near 2.5 eV, accompanied by a decrease of the intensity of the band near 2.12 eV. Any further increase of the iodine concentration leads to a decreasing relative quantum yield of the luminescence as shown in figure 3 and to a long-wavelength shift of the luminescence band. At an iodine concentration of about $2 \times 10^{18} \text{ cm}^{-3}$ the 2.5 eV band is shifted to 2.4 eV. These spectra coincide well with previously reported results (see for example [1, 8]).

The luminescence decay curve at low-power excitation ($N_{abs} \leq 10^{15} \text{ cm}^{-3}$) is the same for nitrogen and dye laser excitation but depends on the iodine concentration. Figure 4 shows examples of pulsed luminescence decay in AgBr crystals with different iodine concentrations, under excitation by a Coumarin dye laser emitting 440 nm giving a surface density excitation of about 10^{14} cm^{-2} . The luminescence decay is exponential with a decay time $\tau_0 = 15.2 \mu\text{s}$ at 20 K in crystals with iodine concentration in the range $4 \times 10^{15} - 1.6 \times 10^{17} \text{ cm}^{-3}$ (figure 4, curve 1). At higher concentrations up to $2 \times 10^{18} \text{ cm}^{-3}$, at which the relative quantum yield decreases, the luminescence pulse also decays exponentially, but with a decay time shorter than that for crystals with low iodine concentration (figure 4, curve 2). At still higher iodine concentrations the luminescence pulse kinetics became more complicated (figure 4, curve 3).

Increasing the excitation power intensity higher than some level, which depends on iodine concentration in the crystal, leads to a saturation of the luminescence pulse intensity. Figure 1 shows the normalized dependence of the relative quantum yield of the iodine bound exciton luminescence on the concentration of absorbed quanta at 440 nm for AgBr crystals with various iodine concentrations. The relative quantum yield was taken as the integral over time of the luminescence pulse divided by the absorbed quanta concentration.

Increasing the pulsed excitation power density leads to luminescence decay changes. This effect is weak in samples with low iodine concentration, even at the highest excitation density. For concentrations of iodine higher than $4 \times 10^{16} \text{ cm}^{-3}$, however, changes in the decay kinetics are much more pronounced. At a moderate excitation intensity the luminescence decay is faster and becomes non-exponential in the initial part. At still higher excitation intensities a fast component of the luminescence pulse appears. Examples of

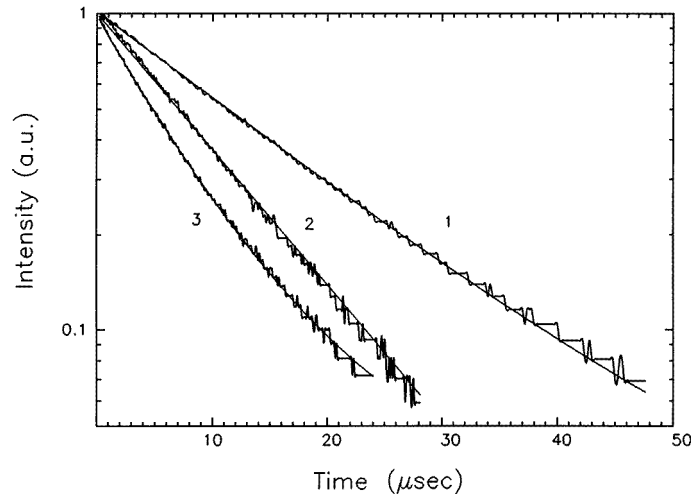


Figure 4. Normalized luminescence decay curves under excitation by a Coumarin 440 dye laser with a surface power density of 10^{14} cm^{-3} for AgBr crystals doped by iodine with concentrations of 4×10^{15} – $1.6 \times 10^{17} \text{ cm}^{-3}$ (curve 1), $2 \times 10^{18} \text{ cm}^{-3}$ (curve 2) and $2 \times 10^{19} \text{ cm}^{-3}$ (curve 3) (a.u., arbitrary units). The solid curves are theoretical approximations of the experimental decay curves.

the normalized luminescence decay curves are shown in figures 5 and 6 for AgBr crystals activated with iodide ion concentrations of 1.6×10^{17} and $2 \times 10^{18} \text{ cm}^{-3}$ and excited by dye or N_2 lasers. At an excitation power where the fast component in the luminescence pulses appears, the spectral distributions of the fast and slow components were measured (figure 7). In these measurements the luminescence pulse was measured on a slow time scale of the oscilloscope and the slow part of the luminescence pulse was approximated by an exponential decay. The fast-component intensity was estimated by subtracting the intensity of the slow component from the initial intensity of the luminescence pulse. It is seen that spectra of the fast and slow components of the luminescence pulses coincide with the luminescence spectra measured under weak continuous excitation of a Xe lamp.

4. Discussion

4.1. Theoretical background

The appearance of the fast component of the luminescence, the shortening of the slow component of the luminescence and the threshold nature of these effects are typical in stimulated luminescence. However, the observed decrease in the relative quantum yield of the luminescence with rising excitation intensity (figure 1) and the absence of a narrowing of the luminescence spectrum of the fast component of the luminescence pulse (figure 7) indicate that the primary reason for the luminescence decay changes may be luminescence quenching at high excitation powers. This quenching may be due to resonant excitation energy transfer from iodine-bound excitons to quenching centres and due to resonant excitation energy migration under identical iodide ions to centres, where this energy is quenched [13–15].

Very similar effects of kinetic changes with various concentration of activators have

been observed in crystals and glasses activated by rare-earth ions [16–19]. These studies showed that the dependence of the luminescence pulse intensity I on time t can be described by the following expression:

$$I(t) = I_0 \exp\{-[t/\tau_{rad} + \Pi(t)]\} \quad (2)$$

where τ_{rad} is the radiation decay time and $\Pi(t)$ is determined by the various non-radiative channels of excitation energy losses at various time intervals t . The function $\Pi(t)$ is expressed by

$$\Pi(t) = \begin{cases} tW_q & \text{at } \begin{cases} t < t_1 \\ t_1 < t < t_2 \\ t > t_2. \end{cases} \\ \gamma t^{0.5} & \\ tW_m & \end{cases} \quad (3)$$

W_q is the probability of the luminescence quenching by quenching centres at the shortest possible distance R_{min} . This exponential portion occurs in the initial part of the luminescence process, $t < t_1$. The later part of the decay curve at $t_1 < t < t_2$ is a luminescence-quenching interaction over different distances R , where γ is determined by the overlap integral of the luminescence spectrum of the luminescence centres and the absorption spectrum of the quenching centres and by the concentration of the quenching centres (the so-called Förster decay law [17]). In the final stage at $t > t_2$ the luminescence pulse decays exponentially. In this time range the decay time is determined by the migrating excitations with probability W_m through luminescence centres to the region of a strong interaction, where they are quenched.

4.2. Low excitation intensities

At low excitation intensities, where the relative quantum yield of the luminescence is not dependent on the excitation intensity (see figure 1), the dependence of the luminescence intensity decay curves on the iodine concentration seems to fall into three ranges. In the concentration range of 10^{17} cm^{-3} or less in which the curve of the luminescence pulse does not change with increasing iodine concentration the luminescence intensity is approximated by the expression

$$I = A_0 \exp(-t/\tau_0) + C \quad (4)$$

where τ_0 is the exponential decay time and A_0 and C represent the relative amplitudes of the exponential part of the luminescence kinetic and slow recombination luminescence which is observed in AgBr crystals [1, 5, 14]. Values of τ_0 , A_0 and C in this concentration range are independent of the iodine concentration and are $15.2 \mu\text{s}$, 0.98 and 0.02 , respectively. The value of $15.2 \mu\text{s}$ for τ_0 differs slightly from the value reported in [1, 2] because of thermal quenching of the luminescence at 20 K. In this concentration range the luminescence is due to radiative transitions in well separated non-interacting iodine-bound excitons. In the concentration range 10^{17} – 10^{18} cm^{-3} the luminescence pulse may also be approximated by equation (4), but τ_{sl} becomes smaller and at a concentration of about $2 \times 10^{18} \text{ cm}^{-3}$ it is equal to $9.8 \mu\text{s}$. In this concentration range the dependence of the relative quantum yield of the luminescence on iodine concentration decreases (figure 2). In the theoretical part of the discussion it is shown that the shortening of the exponential decay time with rising luminescence centres concentration can be explained by excitation energy migration over unexcited identical luminescence centres up to the strong interaction range with quenching centres. In AgBr:I crystals with intermediate iodine concentrations, the process of excitation migration over iodide ions to the quenching centres becomes effective. In this case, the

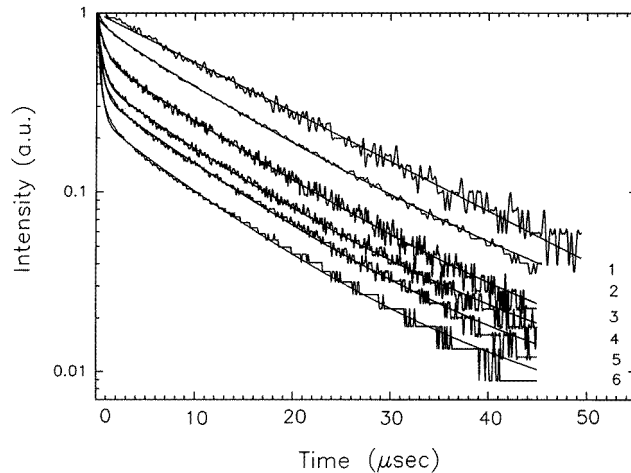


Figure 5. Normalized luminescence decay curves for AgBr crystal with $1.6 \times 10^{17} \text{ cm}^{-3}$ iodine concentration under excitation by dye laser pulses with wavelength 440 nm (curves 1 and 2) and by N_2 laser pulses (curves 3–6) (a.u., arbitrary units). Curves 1 and 2 presents the luminescence pulses with absorbed excitation quanta concentration equal to 10^{15} cm^{-3} and $7 \times 10^{17} \text{ cm}^{-3}$ subsequently. Concentrations of the absorbed excitation quanta for curve 3 are equal to $1.5 \times 10^{19} \text{ cm}^{-3}$, for curve 4 are $2.7 \times 10^{19} \text{ cm}^{-3}$, for curve 5 are $1.2 \times 10^{20} \text{ cm}^{-3}$ and for curve 6 are $3 \times 10^{20} \text{ cm}^{-3}$. The solid curves are a theoretical approximation by equation (6) with the parameters listed in table 2.

luminescence pulse decay time τ_{sl} may be expressed by $1/\tau_{sl} = 1/\tau_0 + 1/\tau_m$, where $1/\tau_m$ is equal to the energy migration probability W_m . At an iodine concentration of $2 \times 10^{18} \text{ cm}^{-3}$, W_m is about $3.6 \times 10^4 \text{ s}^{-1}$. At still higher iodine concentrations, the luminescence decay becomes more complicated and has already been explained by donor–acceptor recombination [5]. The acceptor is a hole localized on the iodide ion and the electron donor centre is an interstitial silver atom [5]. The luminescence decay at this iodine concentration may also be explained by luminescence quenching. In this concentration range, two quenching mechanisms seem to participate in the luminescence process. In the initial stage, luminescence is determined by direct interaction between iodine-bound excitons and quenching centres distributed over distance R . The luminescence decay curve at a later stage is determined by the excitation energy migration over iodide ions to the quenching centres. In this case the normalized luminescence decay curve may be approximated by the expression

$$I(t) = B \exp(-\gamma t^{0.5}) + A_{sl} \exp(-t/\tau_{sl}) \quad (5)$$

where B is the relative concentration of the iodine-bound excitons quenched because of a resonant interaction between excitons and quenching centres distributed over distance R , A_{sl} is the relative concentration of the iodine-bound excitons quenched owing to exciton energy migration to the quenching centres, γ is the interaction parameter between iodine-bound excitons and quenching centres and τ_{sl} is the decay time at the later stage. These concentration-dependent quenching mechanisms of the iodine-bound exciton luminescence at low excitation intensities, which manifest themselves by changes in the luminescence kinetics, are very close to the ideas proposed by Czaja [7]; he observed spectral changes in the zero-phonon line of the iodine-bound exciton luminescence.

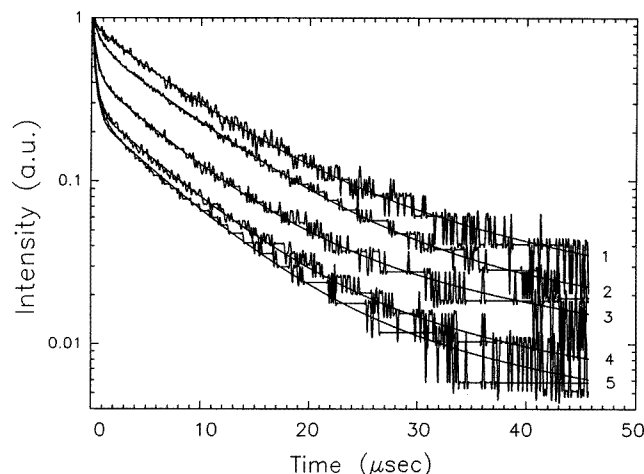


Figure 6. Normalized luminescence decay curves for an AgBr crystal with $2 \times 10^{18} \text{ cm}^{-3}$ iodine concentration under excitation by 440 nm dye laser pulses with an absorbed quanta concentration of 10^{16} cm^{-3} (curve 1) and by N_2 laser pulses with an absorbed quanta concentration equal to $1.7 \times 10^{18} \text{ cm}^{-3}$ (curve 2), $1.3 \times 10^{19} \text{ cm}^{-3}$ (curve 3), $9 \times 10^{19} \text{ cm}^{-3}$ (curve 4) and $3 \times 10^{20} \text{ cm}^{-3}$ (curve 5) (a.u., arbitrary units). The solid curves are theoretical approximations by equation (6) with the parameters listed in table 3.

4.3. High excitation intensities

At high excitation intensities the dependence of the relative quantum yield on excitation power density decreases (see figure 1), and the luminescence decay is not exponential over the entire iodine concentration range measured (see figures 5 and 6). The experimental decay curves of the luminescence pulses at this high-power excitation are well approximated by the expression

$$I(t) = A_{fst} \exp(-t/\tau_{fst}) + B \exp(-\gamma t^{0.5}) + A_{sl} \exp(-t/\tau_{sl}) \quad (6)$$

where the parameter A_{fst} is the relative concentration of the iodide-bound excitons quenched by direct interaction with nearby quenching centres. The best-fit curves of the luminescence pulse shapes to equation (6) are presented in figures 5 and 6 by solid curves and the best-fit parameters obtained for different concentrations of iodine and different intensities of the excitation are listed in tables 2 and 3.

The values of τ_{fst} and τ_{sl} are given by the following equations:

$$\begin{aligned} 1/\tau_{fst} &= 1/\tau_{rad} + 1/\tau_q \\ 1/\tau_{sl} &= 1/\tau_{rad} + 1/\tau_m. \end{aligned} \quad (7)$$

Using these equations, the probability $W_q = 1/\tau_q$ of the luminescence quenching at small distances between bound excitons and quenching centres and the migration probabilities $W_m = 1/\tau_m$ were estimated and listed in table 4.

Changes in the luminescence decay curve begin to be observable at absorbed quanta volume densities (concentrations of electron-hole pairs) higher than the iodine concentration in crystals. It may be thought that, in this excitation intensity range, raising the excitation power density cannot significantly alter the concentration of the iodide-bound excitons. Therefore, observed effects of the luminescence pulse changes cannot be due to luminescence quenching by the interaction between iodine-bound excisions and unexcited

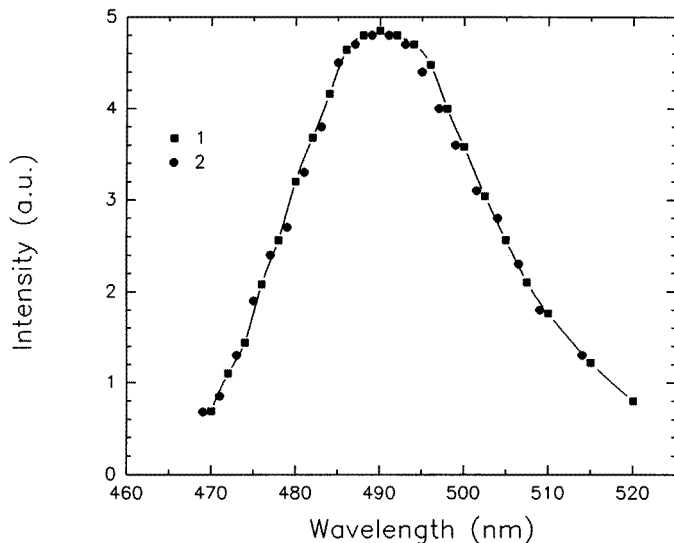


Figure 7. Luminescence spectra of the fast (■) and slow (●) components of the luminescence pulse in AgBr:I crystals with an iodine concentration of $1.6 \times 10^{17} \text{ cm}^{-3}$ at 20 K under excitation by 337 nm N_2 laser pulses (a.u., arbitrary units). The absorbed excitation quanta concentration is $9 \times 10^{19} \text{ cm}^{-3}$.

Table 1. Luminescence decay parameters at low excitation intensities. N_I is the iodine concentration in the crystal; τ_0 and τ_{sl} are the decay times of the exponential part of the luminescence pulse which characterizes radiative probability and energy migration probability, accompanied by quenching; A_0 , A_{sl} is the relative concentration of the iodine-bound excitons which decay exponentially, and B is the relative concentration of the iodine-bound excitons which decay in accordance with Förster's law; γ is the donor-acceptor interaction parameter.

N_I (cm^{-3})	τ_0, τ_{sl} (μs)	A_0, A_{sl}	B	γ ($\text{s}^{1/2}$)
$(4-16) \times 10^{16}$	15.2	1	—	—
2×10^{18}	9.8	1	—	—
2×10^{19}	7.2	0.83	0.17	240

iodide ions as in the case of low excitation intensities and high iodine concentrations. We suggest that in the high excitation intensity range the quenching centres are electron centres, created in the crystal by strong excitation and have absorption spectra in the range of the iodine-bound exciton luminescence [20]. These centres must have relatively short lifetimes because the kinetics and relative quantum yield of the luminescence reset to prior values when the excitation intensity is reduced. If the concentration of the quenching centres is proportional to the concentration N_{abs} of the absorbed excitation quanta, then, in the case of the dipole-dipole interaction, the migration probability W_m to quenching centres should depend linearly on $1/R^6$, where R is the mean distance between quenching centres [13]. Figure 8 shows the dependence of W_m on $1/R^6$ where R is defined as $(\frac{3}{4}\pi N_{abs})^{1/3}$. It can be seen that good agreement is obtained between theory and experiment.

The quenching probability W_q at small distances between iodine-bound excitons and quenching centres also depends linearly on $1/R^6$ (see figure 8, curve 2) and may be explained

Table 2. Luminescence decay parameters at high-power excitation for AgBr crystals with an iodine concentration of $1.6 \times 10^{17} \text{ cm}^{-3}$. The meanings of the parameters τ_{sl} , A_{sl} and B in tables 2 and 3 are the same as in table 1; $1/\tau_{fst}$ is the combined probability of the radiative transitions and quenching probability at close distance between iodine-bound excitons and quenching centres; A_{fs} is the relative concentration of such excitons.

N_{abs} (10^{19} cm^{-3})	τ_{sl} (μs)	τ_{fst} (μs)	A_{sl}	B	A_{fst}	$\gamma \times 10^{-3}$ ($\text{s}^{-1/2}$)
10^{-4} – 10^{-2}	15.1	—	1	—	—	—
7×10^{-2}	12.7	—	0.64	0.36	—	0.33
1.7	11.9	0.71	0.47	0.14	0.39	0.35
2.7	11.2	0.47	0.30	0.17	0.53	0.38
12	10.9	0.42	0.27	0.1	0.62	0.35
30	10.3	0.34	0.19	0.09	0.71	0.37

Table 3. Luminescence decay parameters at high excitation for AgBr crystals with a $2 \times 10^{18} \text{ cm}^{-3}$ iodine concentration.

N_{abs} (10^{19} cm^{-3})	τ_{sl} (μs)	τ_{fst} (μs)	A_{sl}	B	A_{fst}	$\gamma \times 10^{-3}$ ($\text{s}^{1/2}$)
0.001	8.9	—	0.63	0.37	—	0.36
0.17	8.4	0.85	0.62	0.08	0.31	0.20
1.3	6.9	0.4	0.35	0.12	0.53	0.31
9.7	7.0	0.32	0.29	0.06	0.7	0.37
33	6.8	0.28	0.22	0.046	0.74	0.30

Table 4. Energy migration probability W_m and quenching probability W_q determined using equation (7) in crystals with an iodine concentration of $1.6 \times 10^{17} \text{ cm}^{-3}$.

N_{abs} (cm^{-3})	W_m (10^4 s^{-1})	W_q (10^6 s^{-1})
7×10^{17}	1.3	—
1.7×10^{19}	1.8	1.3
2.7×10^{19}	2.3	2.06
1.2×10^{20}	2.6	2.3
3×10^{20}	3.1	2.9

by the distance distribution of the quenching centres in proximity to iodine-bound excitons. This distribution of the closely spaced quenching centres may be due to a large Bohr exciton radius for iodine-bound excitons in AgBr crystals [21].

5. Summary

The spectral and kinetic properties of AgBr:I crystals have been studied as functions of the iodine concentration over four orders of magnitude and as functions of excitation intensity over five orders of magnitude. Raising the iodine concentration or exciton power density quenches the luminescence. This luminescence quenching manifests itself by a reduction in the relative quantum yield of the luminescence, and by changes in the luminescence pulse shape. All observed effects may be explained self-consistently as being due to three types

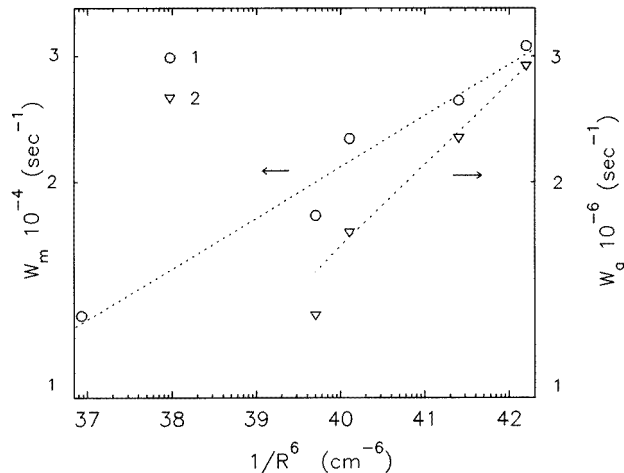


Figure 8. Dependences of the probabilities W_m (\circ) and W_q (∇) on the concentration squared of the absorbed quanta N_{abs}^2 for AgBr crystals with an iodine concentration $1.6 \times 10^{17} \text{ cm}^{-3}$.

of dipole–dipole interaction between the iodide-bound excitons and unexcited iodide ions and between iodine-bound excitons and quenching centres, which are produced by high-intensity excitation. At low-power excitation, quenching effects are explained by excitation energy migration via unexcited iodide ions to the quenching centres and by direct interaction between iodine-bound excitons and quenching centres, distributed over some distance R . At high-power excitation the direct interaction between iodine-bound excitons and quenching centres in the close vicinity explain additional effects observed under high-power excitation.

Acknowledgments

The authors wish to thank F Moser for helpful discussion and A Levite for the production of the crystals.

This work was supported by a grant from the German–Israeli Foundation for Scientific Research and Development, Austrian–Israeli foundation and by a donation from the Raymond and Beverly Sackler Institute of Solid State Physics.

References

- [1] Moser F and Lyu S 1971 *J. Lumin.* **3** 447
- [2] Kanzaki H and Sakuragi S 1969 *J. Phys. Soc. Japan* **27** 109
- [3] Tsukakashi M and Kanzaki H 1971 *J. Phys. Soc. Japan* **30** 1423
- [4] Ueta M, Kanzaki H, Kobayshi K, Yoyozawa Y and Hanamyra E 1986 *Excitonic Processes in Solids (Springer Ser. Solid State Sci.)* (Berlin: Springer) p 60
- [5] Marchetti A and Burberry M 1983 *Phys. Rev. B* **28** 2130
- [6] Czaja W and Baldereschi A 1979 *J. Phys. C: Solid State Phys.* **12** 405
- [7] Czaja W 1983 *J. Phys. C: Solid State Phys.* **16** 3197
- [8] Marchetti A P and Burberry M 1988 *Phys. Rev. B* **37** 10 862
- [9] Kleinfeld Th and von der Osten W 1984 *Phys. Status Solidi b* **125** 293
- [10] Baba T and Masumi T 1976 *Nuovo Cimento B* **39** 609
- [11] Pelant I, Mysyrowicz A and Guillaume B 1976 *Phys. Rev. Lett.* **37** 1708
- [12] Baba T and Masumi T 1987 *J. Phys. Soc. Japan* **56** 2549

- [13] Dexter D 1953 *J. Chem. Phys.* **21** 836
- [14] Imbusch G 1967 *Phys. Rev.* **153** 326
- [15] Förster T 1949 *Z. Naturforsch.* a **4** 321
- [16] Yen W (ed) 1989 *Laser Spectroscopy of Solids II (Top. Appl. Phys. 65)* (Berlin: Springer)
- [17] Voron'ko Yu, Mamedov T, Osoko V, Timoshechkin M and Scherbakov I 1974 *Sov. Phys.-JETP* **38** 565
Voron'ko Yu, Mamedov T, Osoko V, Prokhorov A, Sakun V and Scherbakov I 1976 *Sov. Phys.-JETP* **44**
251
- [18] Strauss E, Miniscalco W, Hegarty J and Yen W 1981 *J. Phys. C: Solid State Phys.* **14** 2229
- [19] Wyatt R 1991 *Optical Fiber Lasers and Amplifiers* ed P France (London: Blackie) p 79
- [20] Kanzaki H 1980 *Photogr. Sci. Eng.* **24** 219
- [21] Marchetti A and Tinti D 1979 *Phys. Lett.* **69A** 353